Hybridization and Enzymatic Extension of Au Nanoparticle-Bound Oligonucleotides

Sheila R. Nicewarner Peña, Surabhi Raina, Glenn P. Goodrich, Nina V. Fedoroff,* and Christine D. Keating*

Contribution from the Department of Chemistry and Life Sciences Consortium, The Pennsylvania State University, University Park, Pennsylvania 16802

Received December 17, 2001

Abstract: We have investigated the impact of steric effects on the hybridization and enzymatic extension of oligonucleotides bound to 12-nm colloidal Au particles. In these experiments, a nanoparticle-bound 12-mer sequence is hybridized either to its solution phase 12-mer complement or to an 88-mer template sequence. The particle-bound oligonucleotide serves as a primer for enzymatic extension reactions, in which covalent incorporation of nucleotides to form the complement of the template is achieved by the action of DNA polymerase. Primers were attached via -C_6H_{12}SH, -$C_{12}H_{24}$SH, and -TTACAATC_6H_{12}SH linkers attached at the 5′ end. Primer coverage on the nanoparticles was varied by dilution with ⁵′HSC_6H_{12}AAA AAA³′. Hybridization efficiencies were determined as a function of linker length, primer coverage, complement length (12-mer vs 88-mer), and primer:complement concentration ratio. In all cases, hybridization for the 88-mer was less efficient than for the 12-mer. Low primer surface coverages, greater particle−primer separation, and higher primer:complement ratios led to optimal hybridization. Hybridization efficiencies as high as 98% and 75% were observed for the 12-mer and 88-mer, respectively. Enzymatic extension of particle-bound primers was observed under all conditions tested; however, the efficiency of the reaction was strongly affected by linker length and primer coverage. Extension of primers attached by the longest linker was as efficient as the solution-phase reaction.

Introduction

Nano- and microscopic particles have considerable potential as amplification and identification tags in biological analysis.[1−14] Colloidal Au nanoparticles, in particular, have found application in a variety of assay formats in which analyte binding is coupled to particle adsorption. Nanoparticle detection is then used to infer the presence of the analyte of interest. This type of

approach has been used to improve detection limits for proteins and DNA in assays based on nanoparticle optical, electrical, and physical properties. Colloidal Au can be synthesized (or purchased) with high monodispersity and is amenable to biomolecule attachment. While protein:Au nanoparticle conjugates have been used for decades, and have found increasingly broad application,[15−17] it is only recently that nucleic acids have been coupled to colloidal Au and shown to retain the ability to selectively and reversibly hybridize to complementary sequences. Mirkin, Letsinger, and co-workers used 5′ and 3′ thiol moieties to prepare DNA oligomer:Au nanoparticle conjugates and have demonstrated a variety of Au nanoparticle-based DNA assays in which absorbance,[18] scattering,[19] and even Ag plating[20] were employed to improve sensitivity. A similar approach has been demonstrated by Köhler et al., who used the optical signal from DNA:Au conjugates to read out micropatterned DNA chips.[21] DNA:Au conjugates have also been used to improve

* To whom correspondence should be addressed. E-mail: keating@chem.psu.edu and nvf1@psu.edu.

(1) Elghanian, R.; Storhoff, J. J.; Mucic, R. C.; Letsinger, R. L.; Mirkin, C. A. *Science* **1997**, *277*, 1078−1081.
(2) Mirkin, C. A.; Letsinger, R. L.; Mucic, R. C.; Storhoff, J. J. *Nature* **1996**, *382*, 607−609.
(3) Chan, W. C. W.; Nie, S. *Science* **1998**, *281*, 2016−2018.
(4) Han, M.; Gao, X.; Su, G. J.; Nie, S. *Nature Biotechnol.* **2001**, *19*, 631−635.
(5) Bruchez, M., Jr.; Moronne, M.; Gin, P.; Weiss, S.; Alivisatos, A. P. *Science* **1998**, *281*, 2013−2016.
(6) Nicewarner-Peña, S. R.; Freeman, G. P.; Reiss, B. D.; He, L.; Peña, D. J.; Walton, I. D.; Cromer, R.; Keating, C. D.; Natan, M. J. *Science* **2001**, *294*, 137−141.
(7) Ye, F.; Li, M. S.; Taylor, J. D.; Nguyen, Q.; Colton, H. M.; Casey, W. M.; Wagner, M.; Weiner, M. P.; Chen, J. *Hum. Mutat.* **2001**, *17*, 305−316.
(8) Walt, D. R. *Science* **2000**, *287*, 451−452.
(9) Battersby, B. J.; Bryant, D.; Meutermans, W.; Matthews, D.; Smythe, M. L.; Trau, M. *J. Am. Chem. Soc.* **2000**, *122*, 2138−2139.
(10) Dunbar, S. A.; Jacobson, J. W. *Clin. Chem.* **2000**, *46*, 1498−1500.
(11) Gerion, D.; Pinaud, F.; Williams, S. C.; Parak, W. J.; Zanchet, D.; Weiss, S.; Alivisatos, A. P. *J. Phys. Chem. B* **2001**.
(12) Taylor, J.; Fang, M. M.; Nie, S. *Anal. Chem.* **2000**, *72*, 1979−1986.
(13) Yguerebide, J.; Yguerabide, E. E. *J. Cell. Biochem. Suppl.* **2001**, *37*, 71−81.
(14) Schultz, S.; Smith, D. R.; Mock, J. J.; Schultz, D. A. *Proc. Natl. Acad. Sci.* **2000**, *97*, 996−1001.

(15) Lyon, L. A.; Musick, M. D.; Natan, M. J. *Anal. Chem.* **1998**, *70*, 5177−5183.
(16) Ni, J.; Lipert, R. J.; Dawson, G. B.; Porter, M. D. *Anal. Chem.* **1999**, *71*, 4903−4908.
(17) Gu, J. H.; Chen, Y. W.; Wang, P.; Ma, J. M.; Lu, S. H. *Supremol. Sci.* **1998**, *5*, 695−698.
(18) Storhoff, J. J.; Elghanian, R.; Mucic, R. C.; Mirkin, C. A.; Letsinger, R. L. *J. Am. Chem. Soc.* **1998**, *120*, 1959−1964.
(19) Taton, T. A.; Lu, G.; Mirkin, C. A. *J. Am. Chem. Soc.* **2001**, *123*, 5164−5165.
(20) Taton, T. A.; Mirkin, C. A.; Letsinger, R. L. *Science* **2000**, *289*, 1757−1760.

detection limits for DNA in surface plasmon resonance, quartz crystal microbalance, and electrochemical assays.[22-25]

In addition to applications in ultrasensitive detection, DNA: Au conjugates have been employed as building blocks for "bottom-up" assembly strategies. Alivisatos and co-workers demonstrated that several nanoscale Au building blocks could be positioned with high accuracy by attaching them to a single long strand of DNA.[26] Niemeyer et al. have synthesized DNA–streptavidin networks that served as scaffolding for the assembly of 1.4-nm Au nanocrystals.[27] Larger DNA–nanoparticle assemblies have been constructed in which two different nanoscale building blocks are alternated based on selective DNA hybridization[28] and in which particle multilayers are built up on a glass substrate by consecutive hybridizations.[29] Recently, DNA hybridization has been used to assemble Au nanoparticles onto patterned substrates prepared by a lithographic approach[30] and by dip-pen nanolithography.[31] DNA complementarity has also been used to direct the assembly of Au wires several hundred nanometers in diameter and several microns long onto planar Au surfaces.[32]

Despite recent research activity in DNA:Au conjugates, we have found only one report of enzymatic manipulation of Au nanoparticle-bound DNA; He et al. used a restriction endonuclease to cut double-stranded DNA linking a Au nanoparticle to a Au film, and observed a decrease in surface plasmon resonance shift associated with particle desorption. While no attempt was made to measure the efficiency of the endonuclease activity, the authors observed that particle desorption was not complete.[22] In contrast, DNA bound to a variety of planar surfaces has been frequently used in ligation, extension, and restriction endonuclease reactions.[33-49] Polymer, glass, or magnetic bead-bound DNA has been enzymatically extended by one or more bases and, recently, PCR amplified.[50-53] Restriction endonucleases have been used to cleave DNA-linked magnetic nanoparticles.[54] Adaptation of these enzymatic processing protocols for use on Au nanoparticles would significantly increase the toolkit available for DNA:nanoparticle applications ranging from sensing to materials assembly. For example, enzymatic extension of a short oligonucleotide bound to a Au particle results in a longer oligonucleotide still bound to the particle. By choice of template, it is possible to predetermine the sequence of the extended particle bound strand; the coverage of long oligonucleotides is determined by the initial primer coverage. After extension the template can be removed by exposure to heat or base, leaving the extended primer strand attached to the nanoparticle. This process allows preparation of DNA:Au conjugates with the high overall coverage of DNA oligomers optimal for conjugate stability[55] while controlling the number and sequence of much longer DNA strands presented to solution. Note that direct adsorption of longer DNA sequences leads to lower coverages and less selective attachment as strand length increases beyond 24 nucleotides (i.e. the relative impact of the thiol–Au interaction on DNA adsorption becomes less significant as the number of potential nucleotide–gold interactions increases).[56]

Enzymatic manipulation of DNA bound to metal nanoparticles presents some challenges not present for DNA on plastic or glass microbeads. For example, the Au–S bond, although thermodynamically stable, is kinetically labile, leading to thiol exchange in the presence of thiol-containing molecules in solution, particularly at elevated temperatures. Buffers used in molecular biology often contain thiols, e.g. dithiothreitol (DTT), that are commonly included as reductants to prevent the formation of disulfide bonds in the enzymes. Note that it is possible to attach DNA to Au nanoparticles via avidin–biotin attachment chemistry, which would avoid the use of thiols altogether.[6,27] We have chosen to work with the thiol chemistry because it affords greater control over linker length and surface coverage. In addition, thiol-based linkers allow closer approach between Au particles and the surface to which they hybridize (e.g. another nanoparticle, a planar substrate) than do avidin–biotin linkers; for detection mechanisms involving optical and electronic coupling, decreased separation can improve sensitiv-

(21) Köhler, J. M.; Csaki, A.; Reichert, J.; Möller, R.; Straube, W.; Fritzsche, W. *Sens. Actuators, B* **2001**, *76*, 166-172.
(22) He, L.; Musick, M. D.; Nicewarner, S. R.; Salinas, F. G.; Benkovic, S. J.; Natan, M. J.; Keating, C. D. *J. Am. Chem. Soc.* **2000**, *122*, 9071-9077.
(23) Zhou, X. C.; O'Shea, S. J.; Li, S. F. Y. *Chem. Commun.* **2000**, 953-954.
(24) Lin, L.; Zhao, H.; Li, J.; Tang, J.; Duan, M.; Jiang, L. *Biochem. Biophys. Res. Commun.* **2000**, *274*, 817-820.
(25) Authier, L.; Grossiord, C.; Brossier, P.; Limoges, B. *Anal. Chem.* **2001**, *73*, 4450-4456.
(26) Alivisatos, P. A.; Johnsson, K. P.; Peng, X.; Wilson, T. E.; Loweth, C. J.; Bruchez, M. P. J.; Schultz, P. G. *Nature* **1996**, *382*, 609-611.
(27) Niemeyer, C. M.; Burger, W.; Peplies, J. *Angew. Chem., Int. Ed.* **1998**, *37*, 2265-2268.
(28) Mucic, R. C.; Storhoff, J. J.; Mirkin, C. A.; Letsinger, R. L. *J. Am. Chem. Soc.* **1998**, *120*, 12674-12675.
(29) Taton, T. A.; Mucic, R. C.; Mirkin, C. A.; Letsinger, R. L. *J. Am. Chem. Soc.* **2000**, *122*, 6305-6306.
(30) Moller, R.; Csaki, A.; Köhler, J. M.; Fritzsche, W. *Nucleic Acids Res.* **2000**, *28*, e91.
(31) Demers, L. M.; Park, S.-J.; Taton, T. A.; Li, Z.; Mirkin, C. A. *Angew. Chem., Int. Ed.* **2001**, *40*, 3071-3073.
(32) Mbindyo, J. K. N.; Reiss, B. R.; Martin, B. R.; Keating, C. D.; Natan, M. J.; Mallouk, T. E. *Adv. Mater.* **2001**, *13*, 249-254.
(33) Liu, Q.; Wang, L.; Frutos, A. G.; Condon, A. E.; Corn, R. C.; Smith, L. M. *Nature* **2000**, *403*, 175-179.
(34) Frutos, A. G.; Smith, L. M.; Corn, R. M. *J. Am. Chem. Soc.* **1998**, *120*, 10277-10282.
(35) Wang, L.; Liu, Q.; Corn, R. M.; Condon, A. E.; Smith, L. M. *J. Am. Chem. Soc.* **2000**, *122*, 7435-7440.
(36) Syvanen, A. C.; Kandegren, U. *Hum. Mutat.* **1994**, *3*, 172-179.
(37) Pirrung, M. C.; Davis, J. D.; Odenbaugh, A. L. *Langmuir* **2000**, *16*, 2185-2191.
(38) Pirrung, M. C.; Connors, R. V.; Odenbaugh, A. L.; Montague-Smith, M. P.; Walcott, N. G.; Tollett, J. J. *J. Am. Chem. Soc.* **2000**, *122*, 1873-1882.
(39) Nilsson, P.; Persson, B.; Uhlen, M.; Nygren, Per-Ake *Anal. Biochem.* **1995**, *224*, 400-408.
(40) Pastinen, T.; Partanen, J.; Syvanen, A. C. *Clin. Chem.* **1996**, *42*, 1391-1397.
(41) Pastinen, T.; Kurg, A.; Metspalu, A.; Peltonen, L.; Syvanen, A. C. *Genome Res.* **1997**, *7*, 606-614.
(42) Nikiforov, T. T.; Rendle, R. B.; Goelet, P.; Rogers, Y. H.; Kotewicz, M. L.; Anderson, S.; Trainor, G. L.; Knapp, M. R. *Nucleic Acids Res.* **1994**, *22*, 4167-4175.
(43) Braun, A.; Little, D. P.; Koster, H. *Clin. Chem.* **1997**, *43*, 1151-1158.
(44) Alfonta, L.; Willner, I. *Chem. Commun.* **2001**, 1492-1493.
(45) Wang, L.; Hall, J. G.; Liu, Q.; Smith, L. M. *Nature Biotechnol.* **2002**, *19*, 1053-1059
(46) Pastinen, T.; Raitio, M.; Lindroos, K.; Tainola, P.; Peltonen, L.; Syvanen, A.-C. *Genome Res.* **2000**, *10*, 1031-1042.
(47) Adessi, C.; Matton, G.; Ayala, G.; Turcatti, G.; Mermod, J.-J.; Mayer, P.; Kawashima, E. *Nucleic Acids Res.* **2000**, *28*, e87.
(48) Broude, N. E.; Woodward, K.; Cavallo, R.; Cantor, C. R.; Englert, D. *Nucleic Acids Res.* **2001**, *29*, e92.
(49) Stevens, P. W.; Hall, J. G.; Lyamichev, V.; Neri, B. P.; Lu, M.; Wang, L.; Smith, L. M.; Kelso, D. M. *Nucleic Acids Res.* **2001**, *29*, e77.
(50) Andreadis, J. D.; Chrisey, L. A. *Nucleic Acids Res.* **2000**, *28*, e5.
(51) Kwiatkowski, M.; Fredriksson, S.; Isaksson, A.; Nilsson, M.; Landegren, U. *Nucleic Acids Res.* **1999**, *27*, 4710-4714.
(52) Tully, G.; Sullivan, K. M.; Nixon, P.; Stones, R. E.; Gill, P. *Genomics* **1996**, *34*, 107-113.
(53) Shumaker, J. M.; Metspalu, A.; Caskey, C. T. *Hum. Mutat.* **1996**, *7*, 346-354.
(54) Perez, J. M.; O'Loughin, T.; Simeone, F. J.; Weissleder, R.; Josephson, L. *J. Am. Chem. Soc.* **2002**, *124*, 2856-2857
(55) Demers, L. M.; Mirkin, C. A.; Mucic, R. C.; Reynolds, R. A., III; Letsinger, R. L.; Elghanian, R.; Viswanadham, G. *Anal. Chem.* **2000**, *72*, 5535-5541.
(56) Steel, A. B.; Levicky, R. L.; Herne, T. M.; Tarlov, M. J. *Biophys. J.* **2000**, *79*, 975-981.

Table 1. Oligonucleotide Sequences Used in This Work

Abbreviation[a]	Sequence (5′ to 3′)	Description
P12	CGC ATT CAG GAT	Primer
N7P12	taa cat tCG CAT TCA GGA T	Primer[b]
A6	AAA AAA	Dilutor
N18	CGA TAA CGG TCG GTA CGG	Non-complementary primer
T12	ATC CTG AAT GCG	First 12 nucleotides of template
N12	TCT CAA CTC GTA	Non-complementary hybridization sequence
T88	TAC GAG TTG AGA ACA CAG ACG TAC TAT CAT TGA CGC ATC AGA CAA CGT GCG TCA AAA ATT ACG TGC GGA AGG AGT TAT CCT GAA TGC G	Template

a C_x before the sequence abbreviation (e.g. C_6P12) denotes the number of CH_2 moieties between the sulfhydryl group and the first nucleotide (i.e. HSC_6H_{12}P12). F added to any of these sequences denotes the presence of a fluorescein moiety (6-FAM). *b* Nucleotides added to the 5′ end of the primer sequence to increase linker length are shown in lower-case letters.

ity. Under the relatively mild reaction conditions used for enzymatic extension (37 °C, ∼1 μM DTT), we observe no thiol exchange.

We report the impact of steric effects on the hybridization and enzymatic extension of Au nanoparticle-bound DNA primers. Variables investigated include (i) the length of linker by which primers were attached to Au, (ii) primer surface coverage, (iii) the ratio of solution-phase complement to the surface-bound primer, and (iv) the length of the solution-phase complement (12-mer or 88-mer). Each of these parameters impacts hybridization to particle-bound oligonucleotides; by optimizing them it was possible to achieve nearly 100% hybridization efficiencies. We found that Au nanoparticle-bound primers could be enzymatically extended to copy an 88-mer template DNA strand under most conditions of linker and spacing, and that both the surface coverage and the linker length of the primers tested were important determinants of extension efficiency. For the longest linker, extension of particle-bound primers was as efficient as the solution-phase process.

Experimental Section

Materials. H_2O used in all experiments was 18.2 MΩ, distilled through a Barnstead Nanopure system. $HAuCl_4 \cdot 3H_2O$ was purchased from Acros. Oligonucleotides used in this work were purchased from Integrated DNA technologies, Inc. (IDT) or the Nucleic Acid Facility (University Park campus). NaCl, NaH_2PO_4, and Na_2HPO_4 were purchased from J. T. Baker Inc. Klenow (the large fragment of DNA polymerase I), REact 2 buffer, and ultrapure agarose were purchased from Life Technologies. Alexa Fluor 488-5-dUTP was purchased from Molecular Probes. Nonlabeled dNTPs were purchased from Promega Life Sciences. Mercaptoethanol (MCE) and dithiothreitol (DTT) were purchased from Sigma. NAP-5 and NAP-10 columns were purchased from Amersham Pharmacia. Bio-Gel P-60 gel, medium grade was purchased from BioRad. MetaPhor agarose was purchased from BioWhittaker Molecular Applications (Rockland, ME).

DNA Sequences Used in This Work. A list of all sequences used in this work is shown in Table 1. We use the following abbreviations to denote 5′ and 3′ functionalization: C_x before the sequence abbreviation (e.g. C_6P12) denotes the number of CH_2 moieties between the 5′ sulfhydryl group and the first nucleotide (i.e. HSC_6H_{12}P12). F added to any of these sequences denotes the presence of a fluorescein moiety (6-FAM). When fluorescein groups were used, they were incorporated at the end of the DNA farthest from the Au particle to minimize any

Scheme 1. Extension from Particle-Bound Primers[a]
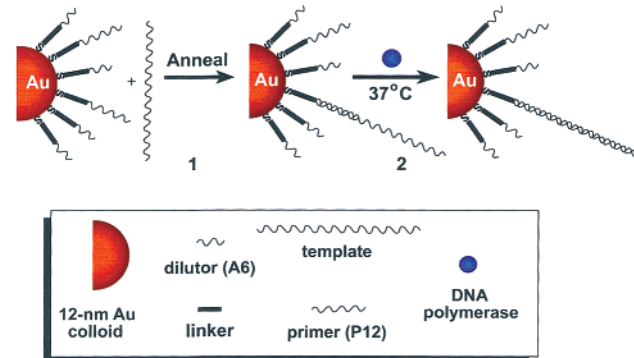
a In step 1, the primers in the DNA:Au conjugates are annealed to the template strand followed by extension in step 2 accomplished by the addition of Klenow (the large fragment of DNA polymerase I).

potential steric interactions. For surface coverage determination experiments, the fluorophore was on the 3′ end, while for hybridization efficiency experiments it was on the 5′ end. Thus, P12F denotes a 3′ fluorophore, while T12F and T88F denote 5′ fluorophores.

Preparation of DNA:Au Conjugates. Surface-diluted conjugates are depicted in Scheme 1. Thiolated oligonucleotides used in this work were received as disulfides. The disulfide was cleaved by using a 100 mM solution of DTT in 0.1 M Na phosphate pH 8.3 buffer. The reaction was allowed to proceed for 30 min at room temperature, after which the oligo was desalted on a NAP-5 or NAP-10 column with elution into autoclaved 18.2 MΩ H_2O. The purified solution of oligonucleotide was quantified with A_{260} and the extinction coefficient specific for the sequence. UV−vis spectra were acquired on a HP 8453 diode array ultraviolet−visible spectrophotometer with 1-nm resolution and 1-s integration time. Colloidal Au particles were prepared by citrate reduction of $HAuCl_4$ as previously described.[57] Transmission electron microscopy (TEM) and Gatan or NIH image[58] software were used to characterize Au nanoparticles. All conjugates used in this work were prepared with the same batch of colloidal Au particles. These particles, referred to throughout the paper as "12-nm", were nearly spherical, having major and minor axes of 13.1 ± 1.3 and 11.0 ± 1.2 nm, respectively.

DNA:Au conjugates were prepared as previously described with a few modifications.[18] In short, 12.5 μL of a 100 μM solution of the oligonucleotide was added to 200 μL of the 12-nm colloidal Au sol. The final concentration of oligonucleotide and colloid was 5 μM and 13.1 nM, respectively. The samples were placed into a water bath at 37 °C for 8 h, after which the solution was brought to 0.1 M NaCl/10 mM Na phosphate pH 7 at a total volume of 500 μL. The samples were left in the "aging" solution for at least 16 h at 37 °C. Following this, samples were centrifuged at 10000g for 40 min, twice, with a rinse of 500 μL of 0.1 M NaCl/10 mM Na phosphate pH 7 in between. Samples were resuspended to a final volume of 200 μL for analysis by fluorescence spectroscopy.

DNA:Au conjugates used in extension experiments were prepared in larger volumes. For these samples, 60 μL of a 100 μM solution of the oligo was added to 140 μL of 18.2 MΩ H_2O followed by addition of 1 mL of the colloidal Au sol. Surface-diluted conjugates were prepared by addition of the primer and the diluent oligo C_6A6 in molar ratios indicated to yield a total oligo solution volume of 60 μL. During "aging", the samples were brought to 0.1 M NaCl/10 mM Na phosphate pH 7 with a total volume of 1.5 mL. Samples were centrifuged twice with a rinse of 1.5 mL of 0.1 M NaCl/10 mM Na phosphate pH 7 between centrifugations. The samples were resuspended into 0.3 M NaCl/10 mM Na phosphate pH 7 for analysis by fluorescence

(57) Grabar, K. C.; Brown, K. R.; Keating, C. D.; Stranick, S. J.; Tang, S.-L.; Natan, M. J. *Anal. Chem.* **1997**, *69*, 471−477.
(58) http://rsb.info.nih.gov/nih-image/; last visited 10/25/01

spectroscopy. A 5-μL sample of each conjugate was taken for quantification of primer concentration, using values determined previously. The final volume of each conjugate was varied so that the final concentration of primer was 3 μM. All DNA:Au conjugates used for extension were quality checked by using a colorimetric solution assay as first described by Mirkin and co-workers.[1]

Fluorescence Quantification of Primer Coverage on Au Particles. Primers used for these studies were labeled with 6-carboxyfluorescein (6-FAM) at the 3′ end. Fluorescently labeled oligos were first adsorbed to the surface of 12-nm diameter colloidal Au particles following the protocol outlined above. For conjugates diluted with C$_6$A6, the primer diluent ratio indicates the ratio of primer to dilutor molecule present in the initial adsorption solution. For the surface-diluted conjugates only the primer oligo was fluorescently labeled. DNA:Au conjugates were washed and centrifuged twice to ensure removal of any nonspecifically adsorbed molecules. The fluorescently labeled oligo was displaced by using 12 mM mercaptoethanol (MCE) as previously described.[55] The conjugates were placed in a 37 °C water bath and left for at least 8 h. The conjugates were then centrifuged again at 10000g for 20 min, after which the supernatant containing the fluorescently labeled oligo was removed and analyzed by fluorescence spectroscopy. Fluorescently labeled oligonucleotides and incorporated fluorescently labeled dUTPs were quantified on a SPEX Fluorolog model 1681 (0.22 m spectrometer) equipped with a PMT.

Hybridization Efficiency of DNA:Au Conjugates. DNA:Au conjugates were prepared as described above and then resuspended into a final volume of 100 μL of 0.3 M NaCl/10 mM Na phosphate pH 7.0. A 5-μL sample from one of each conjugate dilution was removed for visible spectroscopy analysis to determine the concentration of the primer. This was accomplished by determination of the number of Au nanoparticles present based on the A$_{520}$ for each conjugate. Primer concentration was calculated based on the number of Au particles present and the previously determined surface coverage. Conjugates were brought to a final volume of 200 μL for hybridization to 5′ 6-FAM fluorescently labeled complementary oligos T12F and T88F. In this case, the concentration of T12F and T88F was adjusted to maintain the desired primer:complement ratio, while keeping the particle concentration the same in all experiments. The samples were heated in a water bath to 65 °C for 5 min, removed, and allowed to cool to room temperature for 30 min. The conjugates were heated again to 65 °C for 5 min and then allowed to anneal while cooling to room temperature for 120 min in the water bath. After annealing, the conjugates were centrifuged twice at 10000g for 40 min, washing with 500 μL of 0.3 M NaCl/10 mM Na phosphate pH 7 between centrifugations. Conjugates were resuspended into a final volume of 200 μL and the solution pH was brought to 12 by addition of 45 μL of a 1.0 M NaOH solution to dissociate the bound oligonucleotide. The conjugates were placed onto a vortexer with gentle shaking for 2 h. After 2 h, the conjugates were centrifuged again at 10000g for 35 min. The pH of the supernatant was adjusted to 9 with ∼40 μL of a 1.0 M HCl solution (pH was checked with a pH test strip) and analyzed by fluorescence.

DNA Extension from Particle-Bound Primers. A schematic for the extension of particle-bound primers is shown in Scheme 1. Conjugates used in extension reactions were prepared as stated above. Samples for control reactions in which the DNA:Au conjugate primer was noncomplementary to the template were prepared with C$_6$N18. A primer-to-template ratio of 10:1 was used in all experiments. To keep this ratio the same for conjugates that were surface diluted while maintaining the same amount of template molecules in each experiment, the concentration of Au particles for the surface-diluted conjugates was increased such that the primer concentration was kept to 3 μM. Control reactions in which the primer was not attached to the Au particle were carried out by using the same sequence without modification (i.e. N12 and N18). For these reactions, 7.2 μL of a 10 μM solution of N12 or N18 was added to 7.2 μL of a 1 μM solution of N88. For samples in

which the primer was attached to the Au particle, 24 μL of the conjugate was added to 7.2 μL of the template solution. The samples were brought to a final volume of 50 μL with 0.3 M NaCl/10 mM Na phosphate buffer pH 7 for annealing. The reaction mixture was heated to 65 °C for 5 min and allowed to cool to room temperature for 30 min. The sample was again heated to 65 °C for 5 min and allowed to cool to room temperature in the water bath for 2 h. Following annealing of the template to the primer, the reactions were brought to a total reaction volume of 75 μL by addition of 7.5 μL of 10× REact 2 buffer, 11.4 μL nuclease free H$_2$O, 1.1 μL of 50 μM Alexa dUTP, 4 μL of 250 μM dNTPs (150 μM dTTP), and 1 μL of 2U/μL of the DNA polymerase I fragment, Klenow. The samples were placed in a water bath at 37 °C for 2 h for extension. After the allotted time of 2 h, the reaction was quenched by the addition of 4 μL of a 0.5 M EDTA pH 8.0 solution.

After the reaction was quenched, DNA was removed from the particles by displacement with MCE. MCE (1 μL) was added to each sample and allowed to react at 37 °C for 8 h. MCE displaces the thiolated oligonucleotides from the particle surface, a process that leads to particle aggregation. Samples were centrifuged at 10000g for 15 min to pellet the aggregated particles, and the particle-free, DNA-containing supernatant was removed. Prior to purification of samples by column chromatography to remove enzyme and unincorporated dNTPs, 15 μL was removed from each sample and saved for analysis on a MetaPhor agarose gel. The remaining sample was purified by column chromatography with BioRad P-60 gel medium grade. The sample was applied to the column bed. This was followed by 150 μL mobile phase (degassed 0.3 M NaCl/10 mM Na phosphate pH 7); during this time the eluent was sent to waste. Next, 450 μL of the mobile phase was added and the eluent was collected, which contained the dsDNA product. The amount of Alexa Fluor dUTP incorporated was determined by fluorescence spectroscopy with λ_{ex} = 493 nm and λ_{em} = 515 nm. Standards of Alexa Fluor 488-5-dUTP were prepared ranging from 0.7 to 200 nM and run at the time of sample analysis. This was converted into the amount of dTTP incorporated based on the ratio of labeled dUTP to dTTP. From this, the final amount of incorporated nucleotides was calculated based on the number of template molecules added to each reaction mixture.

Samples in which the DNA was not removed from the Au particles were prepared to run on agarose gels as stated above except in the following volumes. Only samples involving conjugates were used in this experiment. A 48-μL aliquot of each conjugate was added to 14.4 μL of the template (T88) followed by addition of 0.3 M NaCl/10 mM Na phosphate pH 7 to bring the total volume for annealing to 75 μL. The total volume for extension was brought to 100 μL by the addition of 10 μL of 10× REact 2 buffer, 9 μL nuclease free H$_2$O, 5 μL of 250 μM dNTPs, and 1 μL of 2U/μL Klenow. Agarose gels, in which the DNA remained on the particles, were scanned into a flatbed scanner and processed with Photoshop, version 5.0. Agarose gels, in which the DNA was removed from the particles, were imaged with a AlphaImager 2200 documentation and analysis system equipped with a CCD and Alpha-Ease image processing and analysis software.

Results and Discussion

Steric factors are expected to play a role both in hybridization to particle-bound oligonucleotides and during enzymatic extension. Indeed, steric effects on extension efficiency may be expected to result not only from decreased extension, but also from decreased hybridization or enzyme binding. Important variables in controlling the steric hindrance experienced by DNA and/or enzyme molecules at the particle surface include the following: (i) the primer surface coverage, (ii) the percentage of primers hybridized, (iii) the distance from the particle surface at which hybridization occurs, and (iv) the length of the complementary sequence. We investigated the effects of each
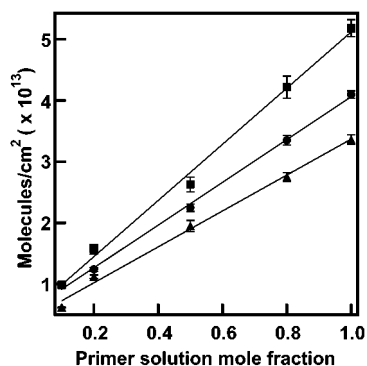
Figure 1. Surface coverage as a function of solution mole ratio for primers C_6P12 (■), $C_{12}P12$ (●), and C_6N7P12 (▲) diluted with C_6A6 and adsorbed to 12-nm diameter Au nanoparticles.

parameter upon hybridization of surface-bound primers to their solution-phase complements, and the effects of primer coverage and linker length upon extension.

Effect of Linker Length and Primer Surface Coverage on Hybridization Efficiencies. The oligonucleotides used to prepare DNA:Au conjugates in this study are of the form HS-linker-primer (see Table 1 for DNA sequences). We investigated three different linkers (C_6H_{12}, $C_{12}H_{24}$, and $C_6H_{12}N7$, abbreviated C_6, C_{12}, and C_6N7, respectively) between the 5′ thiol moiety and the primer sequence (P12). Primer coverage was controlled by competitive adsorption of primers (P12) with a diluent oligonucleotide $HSC_6H_{12}AAA$ AAA. Figure 1 reports the number of particle-bound complementary primers for each linker at solution mole fractions ranging from 0.1 to 1.0. As expected from steric considerations, the C_6 linker gave the highest primer surface coverage, with the longer linkers resulting in somewhat lower coverages in the order of their linker length. Figure 1 also shows that primer coverage is directly proportional to solution mole fraction, in agreement with Demers et al., who report surface dilution of thiolated oligonucleotides with a 20-base polyA sequence on colloidal Au nanoparticles.[55] DNA:Au conjugates were prepared with primer coverages between 6.2×10^{12} and 5.2×10^{13} molecules/cm^2 (28 and 234 molecules/particle).

The importance of both surface coverage and linker length in hybridization efficiency for surface-bound oligonucleotides has been demonstrated on planar surfaces and microbeads.[59−64] For example, Southern and co-workers found the length of linker moieties, rather than their chemical makeup, to be the critical parameter. They recommend linkers of 30 to 60 atoms between a planar substrate and the hybridizing DNA sequence.[59] It has also been demonstrated that decreased oligonucleotide surface coverage leads to improved hybridization efficiencies.[59−64] Although the Au nanoparticles used in this work have a high radius of curvature, which is expected to reduce steric effects, we hypothesized that these parameters would remain important for nanoparticle-bound DNA.
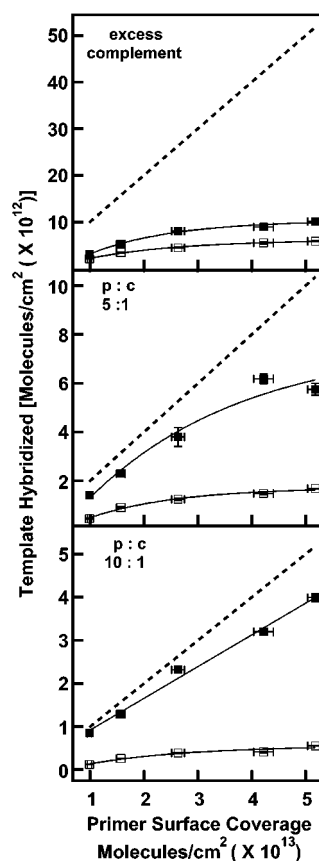
(59) Shchepinov, M. S.; Case-Green, S. C.; Southern, E. M. *Nucleic Acids Res.* **1997**, *25*, 1155−1161.
(60) Southern, E.; Mir, K.; Shchepinov, M. *Nat. Genet. Suppl.* **1999**, *21*, 5−9.
(61) Herne, T. M.; Tarlov, M. J. *J. Am. Chem. Soc.* **1997**, *119*, 8916−8920.
(62) Levicky, R.; Herne, T. M.; Tarlov, M. J.; Satja, S. K. *J. Am. Chem. Soc.* **1998**, *120*, 9787−9792.
(63) Henry, M. R.; Stevens, P. W.; Sun, J.; Kelso, D. M. *Anal. Biochem.* **1999**, *276*, 204−214.
(64) Peterson, A. W.; Heaton, R. J.; Georgiadis, R. M. *Nucleic Acids Res.* **2001**, *29*, 5163−5168.

Figure 2. Effect of particle-bound primer coverage and length of solution-phase complement on hybridization efficiency with three primer-to-complement ratios: excess, 5:1, and 10:1. C_6P12:Au conjugates were hybridized with the complement T12F (■) and the template T88F (□). Solid lines are to guide the eye; dashed lines (- - -) represent 100% hybridization efficiency. Hybridization was quantified by the fluorescence of bound T12F or T88F after removal from the particles (see text for details). As a control, a noncomplementary oligo was used, N12F, for which the fluorescence measurement was below background.

Indeed, Mirkin and co-workers have prepared DNA conjugates with 16-nm diameter colloidal Au nanoparticles, and observed improvements in hybridization efficiency from 4% to 44% with the addition of a 20-base nonhybridizing sequence between the nanoparticles and the 12-mer of interest.[55] The coverage for the longer sequence was substantially less than that for the 12-mer, at 9.0×10^{12} molecules/cm^2 as compared to 2.0×10^{13} molecules/cm^2.[55] This was not unexpected: long DNA strands are known to result in lower surface coverages on planar substrates.[56] The linking sequences used in this work are much shorter, with the longest only C_6N7 (or 49 atoms, ~2 nm). Thus, it was possible to achieve somewhat similar surface coverages with all three linkers, separating the effects of surface coverage and linker length. Maximum coverage for the three primer oligonucleotides ranged from 3.4×10^{13} to 5.2×10^{13} molecules/cm^2 for these linkers.

To determine the accessibility of surface-bound primers for hybridization, we employed both a 12-mer DNA sequence complementary to the primer (T12) and an 88-mer containing the complementary 12-mer at its 3′ end (T88; this sequence is also the template for extension). Figure 2 (top panel) shows the results of hybridization of particle-bound primers (C_6P12) with excess solution-phase complement (T12F and T88F) as a function of primer coverage. A dashed line illustrates the

hybridized strands/cm^2 expected if *every* primer binds a complementary strand from solution. Hybridization efficiencies are higher for the 12-mer sequence as compared to the 88-mer, consistent with the greater steric effects expected for the longer sequence. At high primer coverages, this difference is most significant. A maximum of ~46 or ~26 hybridization events occurred per particle for T12 and T88, respectively, corresponding to 20% and 11% of the ~234 total primers on the particles. However, the hybridization efficiency rose to ~33% and 22% at low primer coverages.

We reasoned that as the concentration of the solution-phase complement decreased below that of the particle-bound primer, steric effects might become less pronounced due to greater spacing between hybridized strands on the particles. Figure 2 shows the effect of primer:complement concentration ratio (p: c) on hybridization of T12 and T88 to particle-bound C$_6$P12. The coverage of hybridized complement is much lower for excess particle-bound primer (p:c 5:1 and 10:1) as compared to experiments in which solution-phase complement was in excess. However, a greater percentage of the solution-phase DNA hybridizes when particle-bound primer is in excess. High p:c ratios can be used to ensure that hybridization of the solution-phase strand goes to completion for ultrasensitive detection or for enzymatic reactions such as extension. The difference between T12 and T88 hybridization is more pronounced under excess primer conditions, as the T12 hybridization efficiency improves more with increasing p:c ratio than does the T88 hybridization. Note that by limiting the concentration of solution-phase complement, it is no longer possible for every primer to bind a complementary strand from solution. The maximum percentage of primers that could hybridize at 5:1 p:c is 20%. To account for this, we have calculated hybridization efficiency based on 100% hybridization of the T12 or T88 sequence for this and all experiments in which the solution-phase complement concentration is limiting. For T12, the percent occupancy of primers is close to 15% with a 5-fold excess of primer, and close to 9% with a 10-fold excess. This corresponds to hybridization efficiencies for T12 of 76% and 88%, respectively. At a 10-fold excess of particle-bound primer, the hybridization efficiency for T12 is largely independent of primer coverage, indicating the decreased importance of steric effects under these conditions.

The effect of linker length on hybridization efficiency at a primer:complement ratio of 10:1 is shown in Figure 3. Again, the longer T88 invariably leads to a lower number of hybridization events than T12. However, the difference in hybridization efficiency between T12 and T88 is linker dependent, and decreases substantially with increasing linker length. For the intermediate-length linker, C$_{12}$, hybridization efficiency is strongly dependent upon primer coverage. For T12, hybridization efficiency increases from 70% to 94% as coverage is decreased from 4.1×10^{13} to 1.2×10^{13} primers/cm^2. A nearly 2-fold difference between T12 and T88 is observed. The C$_6$N7 linker gives optimal efficiencies, at the lowest primer coverage, close to 100% for T12 and 75% for T88. The T88 hybridization data can be fit with a line only for the longest linker (Figure 3 bottom), illustrating the effect of steric crowding at high primer coverages for C$_6$P12 and C$_{12}$P12.

Table 2 summarizes the hybridization efficiency data from the experiments in Figures 2 and 3.[65] These data indicate that,

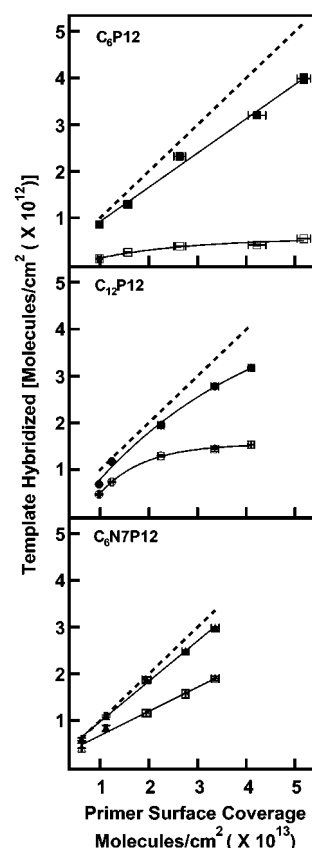**Figure 3.** Effect of linker length and primer coverage on hybridization efficiency at a primer-to-complement ratio of 10:1. C$_6$P12:Au, C$_{12}$P12:Au, and C$_6$N7P12:Au conjugates were hybridized with the complement T12F (closed symbols) and the template T88F (open symbols). Solid lines are to guide the eye; dashed lines (- - -) represent 100% hybridization efficiency. Hybridization was quantified by the fluorescence of bound T12F or T88F after removal from the particles (see text for details). As a control, a noncomplementary oligo was used, N12F, for which the fluorescence measurement was below background.

Table 2. Efficiencies for Hybridization of Particle-Bound Primers to Solution-Phase Complements

linker,[a,b] primer:complement ratio	hybridization efficiency,[c,d] %	
	T12[e]	T88
C$_6$, excess complement	20–33	11–22
C$_6$, 5:1 primer:complement	55–75	17–29
C$_6$, 10:1 primer:complement	76–88	10–17
C$_{12}$, 10:1 primer:complement	70–94	37–59
C$_6$N7, 10:1 primer:complement	89–98	56–75

[a] All primers were P12. See Table 1 for DNA sequences. *[b]* C$_x$ before the sequence abbreviation (e.g. C$_6$P12) denotes the number of CH$_2$ moieties between the sulfhydryl group and the first nucleotide (i.e. HSC$_6$H$_{12}$P12). *[c]* Hybridization efficiencies are calculated based on the concentration of the limiting DNA strand (for excess complement, hybridization efficiency = hybridized primers/total primer strands, while for limiting complement, hybridization efficiency = hybridized complement/total complements). *[d]* Control reactions in which the noncomplementary primer, N18, was used in place of P12; calculated hybridization efficiencies were typically undetectable, and in all cases less than 2%. *[e]* Hybridization efficiencies are calculated from the data in Figures 2 and 3. Because hybridization efficiency is dependent upon primer coverage, a range of efficiencies is given here for each experiment; in all cases, the low end of the range corresponds to high primer coverage and the high end to lower primer coverage.

while steric factors are significant for hybridization of solution-phase complements to nanoparticle-bound primers, these effects can be greatly diminished by decreasing primer coverage and increasing the distance between the primer sequence and the particle surface. For the short solution-phase complement,
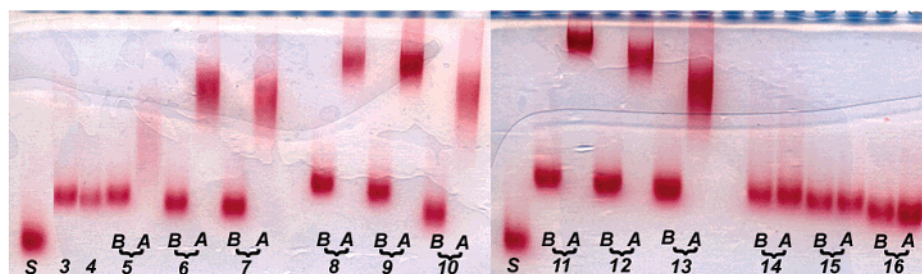
Figure 4. Nondenaturing 3% agarose gel of DNA:Au conjugates used in reactions 3–16 in Table 4. The gel shows conjugates both before (B) and after (A) extension. Conjugates run in lanes labeled "S" were made with C_6A6 and were used as an internal standard. Lanes 3 and 4 which contain C_6P12:Au conjugates are control reactions in which the enzyme and template were omitted, respectively. Lanes 5–7 are reactions that contain C_6P12, lanes 8–10 contain $C_{12}P12$, lanes 11–13 contain C_6N7P12, and lanes 14–16 contain C_6N18:Au conjugates (the noncomplementary control oligo).

hybridization efficiencies approach 100% with the long linkers at low primer coverages and 10:1 primer:complement ratio. While hybridization efficiencies for the long solution phase complement did not reach 100% under these reaction conditions, the importance of linker length, primer coverage, and the ratio of surface-bound to solution-phase oligonucleotides has been demonstrated. In our experiments, the reaction was allowed to proceed for 2 h. This was long enough for complete hybridization between particle-bound primers and T12. However, reaction of the template sequence, T88, may not have gone to completion.

Extension of Particle-Bound Primers. The extension reaction requires not only efficient hybridization of template to the particle-bound primer, but also accessibility to the DNA polymerase enzyme (in this case, the 68 kDa Klenow fragment). Thus, the extension reaction might be expected to show greater sensitivity to steric effects than hybridization alone. Additional concerns include potential nonspecific adsorption of the enzyme to primer:Au conjugates, and deleterious effects of reaction conditions on conjugate stability. In particular, the elevated temperature (37 °C) and trace amounts of the reducing agent, DTT, present during extension might be expected to destabilize the thiol–Au attachment chemistry. To determine the effect of these reaction conditions, conjugates were exposed to various concentrations of DTT at room temperature and at 37 °C. We observed no detrimental effects under our extension reaction conditions.

As an initial test for extension of particle-bound primers, we performed gel electrophoresis on DNA:Au conjugate samples taken before and after the extension reaction. Alivisatos and co-workers recently demonstrated the ability of gel electrophoresis to separate DNA-coated Au nanoparticles based not only on the number of ssDNA molecules attached to each particle but also on the length of the ssDNA.[66] They were able to show separation between DNA:Au conjugates with 50, 80, and 100 base oligomers. Figure 4 shows an unstained agarose gel of our primer:Au conjugates before and after enzymatic extension; bands are visualized by the intense absorbance of the Au particles. Lanes 5–7 contain C_6P12:Au, lanes 8–10 contain $C_{12}P12$, lanes 11–13 contain C_6N7P12, and lanes 14–16 contain C_6N18:Au, the noncomplementary control primer. For each set of conjugates, three surface coverages (corresponding to 100%, 50%, and 20% primer solution mole ratio) were run both before (Figure 4B) and after (Figure 4A) extension.

For all of the complementary primers, a substantial change in electrophoretic mobility is observed upon extension. In all cases the extended conjugates run much slower on the gel, which is consistent with longer DNA bound to the particles. In contrast, no change in band positions was observed for the noncomplementary controls. Note that decreased mobility is not due to particle aggregation; all bands are the red color of isolated Au nanoparticles (as opposed to the blue color of aggregates).[67–69]

The position of each band gives information about the DNA on the particles. The lane marked "S" to the far left of each gel contains C_6A6:Au conjugates as a standard. Lanes 3–5B, which contain C_6P12 at 100% primer coverage, ran significantly slower than "S" because the adsorbed DNA was six nucleotides longer. Note that while this difference in DNA length is much smaller than that distinguished by Alivisatos and co-workers (30 bases),[66] our conjugates harbor many more strands per particle, enhancing differences in electrophoretic mobility. Lanes 6B and 7B also contain C_6P12:Au; however, the primer has been surface diluted with C_6A6 (50% and 20% primer coverage, respectively). Thus, these bands have migrated farther in the gel in proportion to their surface dilution. The same trends can be seen for primers having C_{12} and C_6N7 linkers (lanes 8–10 and 11–13) and for the noncomplementary primer (lanes 14–16). Note that the greater length of these primers results in the lower overall mobility of their conjugates as compared to C_6P12:Au.

While all of the P12 conjugates (lanes 6–13) exhibit substantially decreased electrophoretic mobility upon extension, the *change in mobility* is not equal for all conjugates. For C_6-P12:Au (lanes 5–7), the 50% and 20% coverage conjugates exhibit much greater change in mobility upon extension than the 100% coverage conjugate. If extension had gone to completion on every particle-bound primer, the 100% conjugate band should migrate slower than the 50%, which should migrate slower than the 20%. That this is not observed indicates poor extension efficiency on the high-coverage conjugate. Indeed, this expected band profile is only observed for the longest linker, C_6N7 (lanes 11–13), while the C_{12} linker (lanes 8–10) exhibits intermediate behavior. These data show that both linker length and surface coverage impact the efficiency of extension for particle-bound primers.

(65) In all cases efficiency was calculated based on the maximum possible hybridization events in a given reaction. In cases where primer was limiting (excess template), hybridization efficiency is the fraction of primers hybridized, while for the limiting template (5:1 and 10:1 primer:complement ratio), hybridization efficiency is the fraction of template hybridized.

(66) Zanchet, D.; Micheel, C. M.; J., P. W.; Gerion, D.; Alivisatos, A. P. *Nano Lett.* **2001**, *1*, 32–35.
(67) Storhoff, J. J.; Lazarides, A. A.; Mucic, R. C.; Mirkin, C. A.; Letsinger, R. L.; Schatz, G. C. *J. Am. Chem. Soc.* **2000**, *122*, 4640–4650.
(68) Lazarides, A. A.; Schatz, G. C. *J. Phys. Chem. B* **2000**, *104*, 460–467.
(69) While the early stages of particle aggregation can give optical absorbances very similar to isolated particles, the conjugates in these experiments have been spun down and resuspended several times; any instability would have resulted in substantial aggregation.
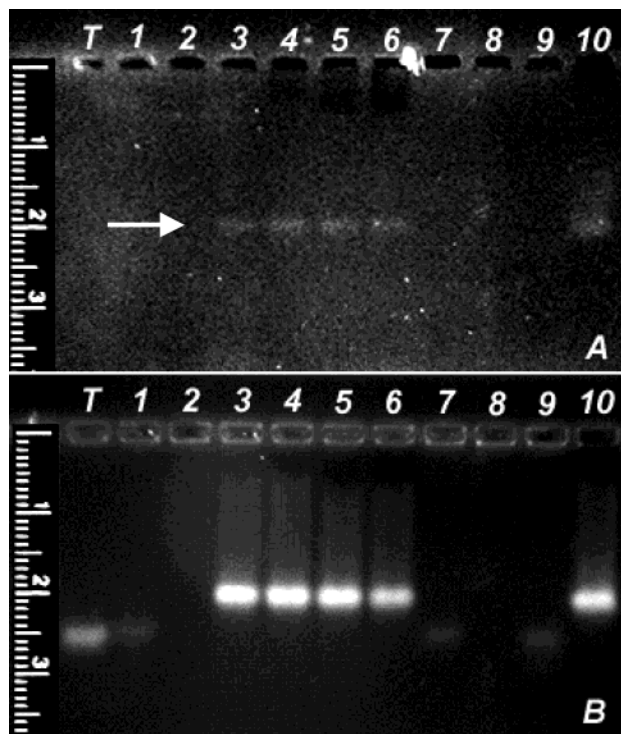
Figure 5. Metaphor 4% agarose gel of reactions 1–10 in Table 3 before (A) and after staining with EtBr (B). The template (T88) was run in lane (**T**) for internal orientation and comparison to the extended products. Evidence for incorporation of the fluorescently labeled dUTP is shown in the gel prior to staining with EtBr (A). The same gel after staining is shown in part B. Lanes 1 and 2 are control reactions in which the enzyme and the template were omitted, respectively. Lane 3 is the solution-phase reaction in which no colloidal Au particles were present in the reaction. Lanes 4–6 are reactions in which increasing amounts of colloidal Au particles are present. Conjugates used in these reactions were made with C_6N18 in concentrations of 100%, 50%, and 20%, respectively. Lanes 7–9 are control reactions for the solution phase in which N18 was used. In lane 7, the enzyme was omitted. In lane 8, the template was omitted. In lane 9, both the enzyme and template were present. Lane 10 was a control reaction in which BSA:Au conjugates were used. Note that the products in lanes 3–6 and 10 are brighter due to the enhanced fluorescence from the Alexa dUTP. The agarose gel was run in 0.5× TBE for 4 h at 3.0 V/cm.

To confirm these observations, we performed the extension reaction in the presence of fluorescently labeled nucleotides and then removed the extended primers from the Au particles for gel electrophoresis and fluorescence quantification. To test for nonspecific adsorption and/or deactivation of Klenow, we added noncomplementary C_6N18:Au or BSA:Au conjugates during solution-phase extension of free primer (P12). Extension was determined by fluorescence of incorporated Alexa Fluor 488-5-dUTP and gel electrophoresis of the extension products. Figure 5 shows a nondenaturing agarose gel before (A) and after (B) staining with ethidium bromide (EtBr). Fluorescence of the incorporated dUTP is observed at ~2 cm (indicated by the white arrow) in lanes 3–6 and 10. These bands correspond to the dsDNA product of the extended primer–template complex. Following staining with EtBr, contrast is much improved and all of the DNA can be imaged (Figure 5B). The double-stranded extension product is now clearly visible for lanes 3–6 and 10. Lane 6 (20% C_6N18:Au) in particular appears to have a lower intensity than the particle-free control (lane 3), indicating a lower extension efficiency. Bands at ~2.6 cm (lanes 1, 7, and 9) correspond to single-stranded template (run in lane T), indicating that no extension occurred in those reactions. The absence of

the ~2.6 cm band in lanes 2 and 8 is expected as no template was added to these reactions.

To address the overall efficiency of extension (i.e. the percentage of template molecules that are copied), quantitative data for fluorescent nucleotide incorporation were acquired. We find a significant (30–40%) decrease in the number of fluorescent dUTPs incorporated when noncomplementary nanoparticle conjugates are present (Table 3). Since there is no difference between the losses for DNA:Au and BSA:Au particles, and since we observe no detectable nonspecific binding in our hybridization experiments, it is unlikely that losses are due to nonspecific adsorption to the particles. The process of removing DNA from the particles involved particle aggregation, centrifugation, and collection of the supernatant for analysis (see the Experimental Section for details). We expect that this process led to significant DNA losses prior to analysis. Some extended DNA may have been trapped in the aggregate, and further losses are expected in removal of the supernatant. Although primer coverage was not expected to significantly affect nonspecific adsorption to DNA:Au conjugates, we ran this control experiment for all three coverages used in the extension experiments because the concentration of Au particles in the reaction was higher for the lower coverage particles (to maintain a constant primer concentration and template concentration for ease of reaction comparison in gels). Thus, at "20% primer" coverage, 5-fold more DNA:Au particles are present than at "100%". We observe decreased efficiency for extension with this increased concentration of Au particles in solution, although the difference is only ~13%. This difference may be due to greater losses during aggregation and centrifugation for samples containing more particles (larger pellet of Au aggregates).

Evidence for extension of particle-bound primers (P12:Au) can be seen in Figure 6A,B, a nondenaturing agarose gel of the extension products run after removal of DNA from the Au nanoparticles. The samples run in each well are described in Table 4. Figure 6A shows the gel prior to EtBr staining; fluorescence from incorporated nucleotides shows up (indicated by the white arrows), albeit weakly, in the wells corresponding to specific primer:Au. After staining with EtBr, contrast is much improved (Figure 6B). Bands present at ~1.9 cm (lanes 1, 5–13) correspond to the double-stranded extension product, while those at ~2.4 correspond to the template. Thus, extension of the particle-bound primer was successful for all linkers and primer coverages attempted. Note that the bands in lanes 11–13 run slightly more slowly than the other dsDNA products. This can be explained by the longer linker (C_6N7) used in these reactions. No extension is observed for the noncomplementary controls (lanes 14–16). The brightness of the extended product band for lanes 5–13 (the various particle-bound primers) is not constant. This indicates some difference in efficiency between the different linker and coverage conditions.

To quantify extension, DNA was removed from the Au nanoparticles and fluorescence from incorporated Alexa-dUTPs was measured (Table 4).[70] The resulting extension data largely follow the same trends for primer coverage and linker length as observed in the hybridization experiments. For the shorter linkers, extension efficiency is lower and the effect of primer coverage is particularly important. As observed for hybridization, extension is most efficient for low primer coverage. In

Table 3. Control Reactions for This Primer:Template System[a]

rxn	sample[a,b]	% NC primer on Au[b,c]	enzyme present	template present	nucleotides recovd in high MW DNA[c,d]	normalized nucleotides recovd[d,e]
1	P12	N/A	−	+	0	0
2	P12	N/A	+	−	0	0
3	P12	N/A	+	+	$1.19 \pm 0.05 \times 10^{14}$	100.0 ± 4.1
4	P12 + C_6N18:Au	100%	+	+	$8.33 \pm 0.13 \times 10^{13}$	70.0 ± 1.1
5	P12 + C_6N18:Au	50%	+	+	$7.59 \pm 0.05 \times 10^{13}$	63.8 ± 0.4
6	P12 + C_6N18:Au	20%	+	+	$7.28 \pm 0.24 \times 10^{13}$	61.2 ± 1.9
7	N18	N/A	−	+	0	0
8	N18	N/A	+	−	0	0
9	N18	N/A	+	+	$4.26 \pm 0.7 \times 10^{11}$	0.4 ± 0.1
10	P12 + BSA:Au	N/A	+	+	$8.29 \pm 0.19 \times 10^{13}$	69.7 ± 1.6

[a] Reactions 1, 2, 7, and 8 were negative controls used to determine background counts for fluorescence quantification. Reactions 1 and 2 contained primer P12 noted in Table 1, while reactions 7 and 8 contained a noncomplementary primer (N18). Reactions 4−6 were performed to determine the efficiency of extension in the presence of increasing amounts of colloidal Au present in the reaction, as this will be necessary to keep the primer-to-template ratio equal for future experiments. Conjugates used in these reactions were made with the C_6N18. [b] C_x before the sequence abbreviation (e.g. C_6P12) denotes the number of CH_2 moieties between the sulfhydryl group and the first nucleotide (i.e. HSC₆H₁₂P12). [c] The % noncomplementary (NC) primer on Au refers to the molar ratio of the primer to the diluent at the initial time of conjugate preparation and is close to the primer/diluent ratio of the final product since the primer vs diluent coverage is nearly linear as shown in Figure 1. [d] The values listed for nucleotides recovered in high MW DNA refer to the total number of nucleotides recovered in the reaction (i.e. incorporated into high MW as a result of extension), and were calculated based on the amount of incorporated Alexa dUTP after purification on P60 columns as determined based on a standard curve. [e] The normalized nucleotides recovered were determined by assigning a value of 100% to the nucleotides recovered in reaction 3, the solution-phase positive control reaction.
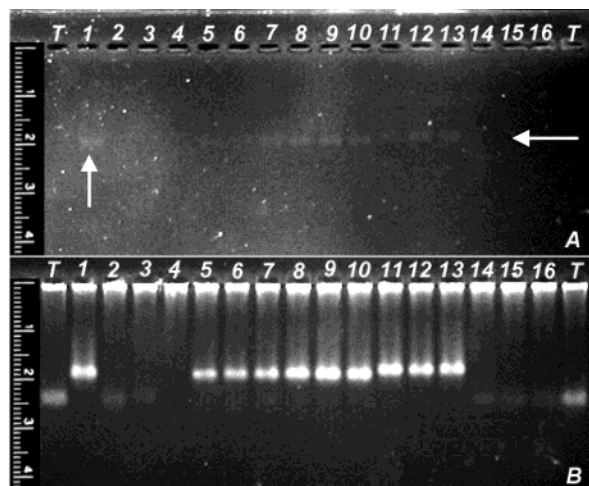

Figure 6. Metaphor 4% agarose gel of reactions 1−16 in Table 4 before (A) and after staining with EtBr (B). The template (T88) was run in lane (**T**) for internal orientation and comparison to the extended products. Evidence for incorporation of the fluorescently labeled dUTP is shown in part A, which is the gel prior to staining with EtBr. The same gel after staining is shown in part B. Lane 1 and lane 2 (negative control) are the solution-phase reactions in which no colloidal Au particles were present. Lanes 3 and 4 are control reactions in which the enzyme and the template were omitted, respectively. Lanes 5−13 are reactions in which the complementary primer:Au conjugate was used, and lanes 14−16 are reactions with C_6N18:Au conjugate. In all cases, conjugates are from lowest colloidal Au concentration to highest, i.e., 100%, 50%, and 20% primer mole fraction. Lanes 5−7 contain C_6P12, lanes 8−10 contain C_{12}P12, and lanes 11−13 contain C_6N7P12. Note that the products in lanes 1 and 5−13 are brighter due to additional fluorescence from Alexa dUTP. The agarose gel was run in 0.5× TBE for 4 h at 3.0 V/cm.

contrast, for C_6N7, this trend is reversed, with the *highest* primer coverage yielding the most efficient extension (71%). This result can be understood in light of the data in Table 3, which illustrate the detrimental effect of higher particle concentrations on

---

(70) The low, but detectible, incorporation observed for the noncomplementary control may result from partial annealing of two template molecules, with one acting as the "primer" for the other. Our column purification step separated oligonucleotides from unincorporated dNTPs but did not separate extended primers from templates, thus any incorporated Alexa-dUTPs are counted as "extended". Note that the probability that two template molecules would anneal *in the presence of the complementary primer* is low because the primer was present in 10-fold excess, and the primer−template complex has higher thermodynamic stability.

solution-phase extension efficiency, presumably due to greater losses in the precipitation/centrifugation step. To maintain constant primer and template concentrations as the primer coverage was decreased, more particles were added to the reaction. Thus, the decreased efficiency resulting from greater particle concentrations may be masking the effect of primer coverage on extension efficiency. Figure 7 plots the extension efficiencies of the data from Table 4 with values normalized to the appropriate control reaction in Table 3.[71] We find that extension efficiency is near 100% for the C_6N7 linker regardless of primer coverage. That is, attachment of the primer to the Au particle has had no effect on the incorporation of fluorescent dUTPs as compared to the free primer in the presence of BSA: Au or noncomplementary N18:Au particles. This was somewhat unexpected given the maximal hybridization efficiency of 75% observed for this primer:template pair (Table 2). Indeed, the extension efficiencies in Figure 7 are in all cases higher than the corresponding template hybridization efficiencies in Table 2. The apparent discrepancy can be understood based on the presence of the enzyme in the extension reaction. While the T_m for this primer−template complex is 36 °C, the enzyme provides stability during extension in two ways. The enzyme drives the annealing of the primer−template complex by latching onto the complex. Further stability is provided by extension of the primer, resulting in a higher T_m duplex. This would lead to greater hybridization efficiencies, making possible the unexpectedly high extension efficiencies.

Conclusions

The hybridization of particle-bound oligonucleotide primers has been determined as a function of linker length, surface coverage, and the ratio of particle-bound to free DNA for both 12-mer and 88-mer solution-phase complements. We find that although steric factors are significant for hybridization to particle-bound primers, hybridization efficiency can be greatly improved by decreasing primer surface coverage, increasing the spacing between the primer sequence and the particle surface,

---

(71) For example, after normalization to the particle-free control within each experiment, the observed efficiency for C_6N7P12 at the highest primer coverage, reaction 11, was divided by the observed efficiency for the corresponding concentration of noncomplementary N18:Au particles, reaction 4 in Table 3.

Table 4. Quantification of Enzymatic Extension from Au-Bound Primers[a]

rxn	sample	% primer on Au[a,b]	enzyme present	template present	nucleotides recovd in high MW DNA[b,c]	normalized nucleotides recovd[c,d]
1	P12	N/A	+	+	$6.21 \pm 0.02 \times 10^{13}$	100.0 ± 2.9
2	N18	N/A	+	+	$2.46 \pm 0.64 \times 10^{12}$	4.8 ± 1.1
3	C_6P12:Au	100%	−	+	0	0
4	C_6P12:Au	100%	+	−	0	0
5	C_6P12:Au	100%	+	+	$1.25 \pm 0.28 \times 10^{13}$	20.2 ± 4.7
6	C_6P12:Au	50%	+	+	$1.90 \pm 0.13 \times 10^{13}$	31.6 ± 3.3
7	C_6P12:Au	20%	+	+	$2.41 \pm 0.08 \times 10^{13}$	41.1 ± 1.4
8	C_{12}P12:Au	100%	+	+	$2.43 \pm 0.09 \times 10^{13}$	40.4 ± 0.7
9	C_{12}P12:Au	50%	+	+	$2.72 \pm 0.05 \times 10^{13}$	45.5 ± 1.1
10	C_{12}P12:Au	20%	+	+	$3.29 \pm 0.17 \times 10^{13}$	54.1 ± 2.8
11	C_6N7P12:Au	100%	+	+	$4.56 \pm 0.15 \times 10^{13}$	73.0 ± 4.2
12	C_6N7P12:Au	50%	+	+	$4.03 \pm 0.30 \times 10^{13}$	65.7 ± 4.8
13	C_6N7P12:Au	20%	+	+	$3.76 \pm 0.06 \times 10^{13}$	61.6 ± 1.2
14	C_6N18:Au	100%	+	+	$3.06 \pm 1.84 \times 10^{11}$	0.4 ± 0.8
15	C_6N18:Au	50%	+	+	0	0
16	C_6N18:Au	20%	+	+	0	0

[a] DNA extension comparing the enzymatic efficiency of particle-bound primers to free primers as well as the effect of spacer length between the primer and the gold particle, and localized concentration of primer, on the gold particle, on enzymatic efficiency. Extension was achieved with T88 as the template and Klenow for enzymatic extension for 2 h at 37 °C. Quantification of incorporated nucleotides was determined via Alexa Fluor 488-5-dUTP, using a fluorimeter. [b] The % primer on Au refers to the molar ratio of the primer to the diluent at the initial time of conjugate preparation. [c] The values listed for nucleotides recovered in high MW DNA refer to the total number of nucleotides recovered in the reaction volume (i.e. incorporated into high MW as a result of extension), and were calculated based on the amount of incorporated Alexa dUTP after purification on P60 columns and were determined based on a standard curve. [d] The normalized nucleotides recovered were calculated based on the nucleotides recovered for the high MW DNA product and the moles of template added to each reaction. These values were normalized to the results of reaction 1.
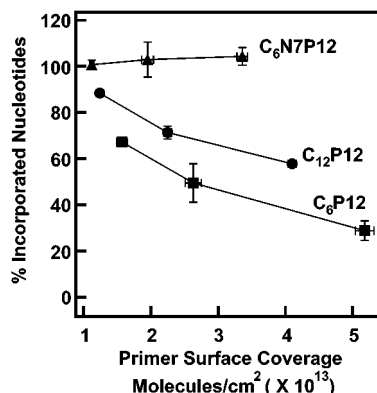

Figure 7. Comparison of enzymatic efficiency on differing linker and primer lengths as well as primer surface coverage of particle-bound primers. Extension was achieved with T88 as the template and Klenow for enzymatic extension for 2 h at 37 °C. Quantification of incorporated nucleotides was determined via Alexa Fluor 488-5-dUTP, using a fluorimeter.

and increasing the ratio of particle-bound primers to their solution-phase complement. In all cases hybridization of the 12-mer complement was more efficient than that of the 88-mer, with optimal hybridization efficiencies of 98% and 75%, respectively. Extension of Au nanoparticle-bound primers by DNA polymerase has been demonstrated. Extension efficiencies as high as 100% were observed for primers bound to Au nanoparticles via a C_6N7 linker. Primers with shorter linkers exhibit a strong dependence on primer surface coverage, and in every case result in less nucleotide incorporation. However, extension was less affected by steric factors than was hybridization alone. This result, while counterintuitive, can be rationalized on the basis that enzyme binding and primer elongation drives hybridization in the extension reactions.

We have for the first time described the enzymatic extension of gold nanoparticle-bound nucleic acids. We find that steric effects remain important, despite the high radius of curvature of the Au nanoparticles used as supports. The factors determined to be important here (linker length, surface coverage) are expected to be generally applicable for all enzymatic reactions on nanoparticle-bound nucleic acids. In addition to extension, it should be possible, for example, to reverse transcribe cDNA onto particles, facilitating gene expression studies, or PCR amplify DNA from Au-bound primers, for subsequent nanoparticle-amplified detection.